Novel bioassays based on 3D-printed device for sensing of hypoxia and p53 pathway in 3D cell models

Novel bioassays based on 3D-printed device for sensing of hypoxia and p53 pathway in 3D cell models

Maria Maddalena Calabretta[a,b*], Maura Ferri[c], Annalisa Tassoni[c], Stefania Maiello[a], Elisa Michelini[a,b,d*]

[a]*Department of Chemistry "Giacomo Ciamician", University of Bologna, Via P. Gobetti 85, 40129, Bologna, Italy*

[b]*Center for Applied Biomedical Research (CRBA), Azienda Ospedaliero-Universitaria Policlinico S. Orsola-Malpighi, 40138 Bologna, Italy*

[c]*Department of Biological, Geological and Environmental Sciences, University of Bologna, Bologna, Italy*

[d]*IRCCS Azienda Ospedaliero-Universitaria di Bologna,40138 Bologna, Italy*

*Corresponding authors:

Prof. Elisa Michelini

University of Bologna

Dept. of Chemistry "Giacomo Ciamician"

Via P. Gobetti 85, 40129 Bologna, Italy

elisa.michelini8@unibo.it

Dr. Maria Maddalena Calabretta

University of Bologna

Dept. of Chemistry "Giacomo Ciamician"

Via P. Gobetti 85, 40129 Bologna, Italy

maria.calabretta2@unibo.it

Abstract

Cell-based assays are widely exploited for drug screening and biosensing, providing useful information about bioactivity of target analytes and complex biological samples. It is well recognized that 3D cell models are required to achieve highly valuable information, also in perspective of replacing animal models. However, bioassays relying on 3D cell models are generally highly demanding in terms of facilities, equipment, and require skilled personnel. To reduce cost, increase sustainability and provide a flexible 3D cell-based platform for bioassays we here report a novel approach based on a 3D-printed microtissue device. To assess the suitability of this strategy for reporter gene technology we selected to monitor two molecular pathways which are of interest in several applications, hypoxia signaling and p53 pathway. The investigation of such pathways is highly relevant in fields spanning from drug screening to bioactivity monitoring for industrial byproducts valorization. Microtissues of human hepatocarcinoma (HepG2) and human embryonic kidney (Hek293T) cell lines were obtained with a low-cost and sustainable chip platform and bioassays were developed to monitor the Hypoxia-Inducible Factors (HIFs) transcription factors and the p53 tumor suppressor pathway. HepG2 and Hek293T 3D cell models were genetically engineered to express the Luc2P from *Photinus pyralis* firefly either under the regulation of p53 or HIF response elements. The bioassays allowed quantitative assessment of hypoxia and tumoral activity with 1,10 phenanthroline for HIF and with doxorubicin for p53 pathway activation, respectively, showing a good potential for applications of this sustainable and low-cost 3D printed microfluidic platform for bioactivity analyses, drug screening and precision medicine.

Keywords: 3D cell model, bioluminescence, bioactivity, 3D-printed device, p53, hypoxia

1. Introduction

The USA and the European Union strongly encourage the use of new *in vitro* assays and in silico methods to replace animal testing in accordance with the Rs principles of Russell and Burch [1]. To identify new compounds with potential bioactivity able to interact with molecular targets and to unravel intra- and inter-cellular signalling in tumoral progression, 3D models represent an invaluable tool for drug discovery programs [2]. Several efforts are focusing on the obtainment of 3D models of either human healthy tissues or diseases to understand molecular mechanisms and to assess the efficacy of novel compounds also on patient-derived cells for personalized medicine [3, 4,5].

Besides drug screening other needs are emerging, such as the availability of rapid and low-cost methods to assess bioactivity of upcycling agro-industrial by-products and food waste [6]. In the last years several agro-food byproduct derivatives have been proposed for food, feed, and nutraceutical applications[7, 8]. The United Nations Agenda 2030 Sustainable Development Goal 12 (SDG 12) - Ensure sustainable consumption and production patterns- aims substantially to reduce waste generation through prevention, reduction, recycling [9].

Several efforts are currently focused on the identification of new routes of circular economy to obtain novel padded value products especially for the pharmaceutical, nutraceutical [10, 11], and cosmetic sectors. In this context the availability of affordable methods for evaluating the bioactivity of byproducts would be highly valuable. 3D cell-based assays that are currently prerogative of preclinical drug discovery because of their high cost and need for sophisticate equipment, would be extremely useful in other fields such as agro-food and industrial waste upcycling. In particular several natural products and agro-food byproducts have been reported having anti-tumoral activity [12] and interesting inhibition of hypoxia-inducible factor (HIF), which responds to decreases in available oxygen [13]. Tissue hypoxia is a pathological condition able to compromise biological cell functions and is caused by inadequate oxygen supply. Solid tumours are characterized by poor blood supply with aberrant vascularization resulting in regions with permanent or transient hypoxic conditions [14].

This leads to the activation of the hypoxia signaling pathway predominantly governed by HIF, that induces several cellular responses to reprogramme cell metabolism, activate inflammation, and help the adaption and progression of tumoral cells to the hypoxic microenvironment [15–17]. A close and complex interplay occurs between the p53 and the hypoxia signalling pathways, impacting tumour progression. The p53 transcription factor works through transcriptional regulation of its target genes, generally in normal cells and tissues under non-stressed conditions p53 protein is present at low levels, conversely in presence of stress signals as well as DNA damage and hypoxia, its protein half-life is dramatically increased leading to its accumulation and activations in cells[18]. Different mammalian cell-based assays have been developed for drug discovery against HIF-1, but their use is limited compared to assays based on genetically engineered bacteria or yeast [19]. In addition, for studying hypoxia cancer biology, two-dimensional *in vitro* models present some limitations to reproduce the spatial heterogeneity and oxygen gradients like in *in vivo* solid tumours [20].

Exploiting bioluminescence (BL) as detection principle, many cell-based assays have been developed to study the bioactivity of natural extracts derivatives and byproducts [21, 22] contributing to the 4Rs principle to reduce, reuse, recycle, and recover of the circular economy [23]. In addition, BL powerful bioanalytical tools have been developed for drug screening assay, also at early-stage level, and to study protein-protein interactions [24]. Moreover, thanks to the availability of a wide luciferase portfolio characterized by high stability, with different wavelengths and kinetic emissions, multiplexed analysis can be performed to simultaneously monitor multiple targets and mechanisms of actions [25, 26]. One of the main advantages of BL in bioanalytical assays is the high signal to noise ratio, the absence of phototoxicity and photobleaching in comparison to fluorescence (FL)-based technique.

Advanced technologies coupled with BL bioanalytical tools [27, 28] are expected to provide new cost-effective and tissue-on-a chip platforms for drug discovery and precision medicine [29–31].

Here we report a novel hypoxia and tumoral sensing in microtissue obtained with a low-cost and sustainable chip platform to assess HIF and p53 pathway activation in 3D spherical microtissues. We decide to focus on HIF and p53 pathway activations which are a pivotal role in tumour development, acting as crucial players in cancer initiation and progression.

To this end, microtissues of Hepatocarcinoma (HepG2) and human embryonic kidney (Hek293T) cell lines were obtained in a microfluidic chip[29] and genetically engineered to express the luciferase Luc2P from the North American firefly *Photinus pyralis* either under the regulation of p53 or HIF response element, respectively.

The analytical performance of the microtissue on a chip-based bioassay was evaluated with 1,10 phenanthroline for HIF activation and with doxorubicin for p53 pathway activation, supporting future potential applicability for bioactivity analyses, drug screening, and cancer precision therapies.

2. Materials and Methods

2.1 Chemical, reagent and instrumentation

Hepatocellular carcinoma (HepG2) and Human embryonic kidney (HEK293T) cells were from ATCC (American Type Culture Collection [ATCC], Manassas, VA, USA). All materials for cell culture maintenance were from Carlo Erba Reagents (Cornaredo, Milano, Italy). Doxorubicin (DOX) and 1,10-phenanthroline, MicroTissues® 3D Petri Dish® micromold spheroids size L 7x5 array, and all other chemicals were purchased from MERCK (St. Louis, MO, USA). The mammalian expression plasmids pGL4.42[luc2P/HRE/Hygro] and pGL4.38[luc2P/p53 RE/Hygro] carrying Luc2P luciferase under the regulation of the hypoxia (HRE) and p53 (p53 RE) response elements, plasmid

extraction kits, beetle luciferin potassium salt (D-luciferin) and BrightGlo substrate were from Promega (Madison, WI, USA). Bioluminescence measurements were performed with Varioskan Flash multimode reader (ThermoFisher Scientific) and with Tecan Microplate Reader Spark® (Tecan Trading AG, Männedorf, Switzerland). The fabrication of the 3D printed microfluidic chip composed by clear biocompatible resin has been previously described [29].

2.2 Luc2P characterization

Luc2P luciferase from *Photinus pyralis* was characterized in terms of emission kinetics and spectra in 2D cell culture, using both the non-lysing D-LH_2 substrate (1.0 mM, pH 5.0) and the commercial BrightGlo substrate. HEK293T were previously seeded in a clear 24-well plate at a density of 8.0×10^4 cells/well, and then transiently transfected with pcDNA3.1-Luc2P, expression vectors using the FUGENE® HD transfection reagent at a ratio of 1:3. Then cells were incubated for 24 h at 37 °C and 5% CO_2. BL measurements were performed with a conventional luminometer Tecan Microplate Reader Spark® after injection of 100 µL of 1.0 mM D-luciferin citrate solution, pH 5.0 or 100 µL of the lysing BrightGlo substrate.

2.3 Tumoral sensing in spherical microtissue

HepG2 cells were grown routinely in 5% CO_2 in air in minimum essential medium with Earle's salts (MEM) supplemented with 10% (v/v) fetal bovine serum, 2 mM L-glutamine, 0.1 mM non-essential amino acids, MEM vitamins, and antibiotic/antimycotic solution.

Cells, previously seeded in a flat-bottom clear 24-well plate at a density of 8.0×10^4 cells/well, were transiently transfected with pGL4.38[luc2P/p53 RE/Hygro], using the FUGENE® HD transfection

reagent at a ratio of 1:4.5 and incubated under standard conditions for 24 h at 37 °C and 5% CO_2. The development of 3D spherical microtissues through self-assembly in a non-adhesive agarose gel were obtained using a 5 × 7 array micromold with 800 μm diameter rounded pegs (3D Petri Dish®, MicroTissues Inc., St. Louis, MO, USA). A 2% w/v agarose solution in 0.9% w/v NaCl was prepared and used to pipet into the micro-mold (330 μL) until gelled, then the agarose gel was separated from the micro-mold and transferred to the holder of microfluidic chip previously developed [29]. To equilibrate the 3D Petri Dish® in the organ-on-a-chip platform, ~6 mL of fresh cell culture medium was pumped through the fluidic inlet and outlet ports connected to micro peristaltic pumps (RP-Q2 miniature peristaltic pump, Takasago Electric, Inc., Nagoya, Japan) using a nominal flow rate of 200 μL min^{-1}. After mold equilibration, the medium was completely removed by the outlet port, cells previously transfected the day before in a clear 24-well plate were detached, counted and seeded in the 3D Petri Dish (3.5×10^4 cells /75 μL) for the obtainment of spheroids with a diameter of about 180 ± 20 μm. The time needed to set the cells by microgravity, ~2.5 mL of fresh medium was pumped with a nominal flow rate of 100 μL min^{-1}. After spheroids formation, the pumps were activated to replace the medium in the container or provide the sample to be analysed.

For monitoring p53 pathway activation doxorubicin solutions were tested (concentration range from 0.0 to 5.0 μM) and incubated for 18 h in standard conditions (37°C, 5% CO_2).

For performing BL measurements, the holders were transferred in a clear 24-well plate after the treatment and emissions kinetics were acquired by adding the commercial lysing BrightGlo substrate (50 μL) and acquiring the signal with a luminometer (Varioskan™ LUX multimode microplate reader) for 10 min with 500 ms integration time. Corrected BL signal was plotted as fold response over the doxorubicin control. Limit of detection (LOD) and limit of quantification (LOQ) were calculated as the doxorubicin concentration that corresponded to the blank plus three times and ten

times the standard deviation, respectively. All measurements were performed in triplicate and repeated at least three times. The half maximal effective concentration (EC50), which is the concentration of the doxorubicin producing 50% of the maximum response, was calculated using the equation: Y = Bottom + (Top − Bottom)/(1 + 10^((LogEC50 − X) × Hillslope)), where X is the logarithmic concentration of doxorubicin.

Repeatability performance of the 3D tumoral sensing assay was calculated as Coefficient of Variation (CV%) = standard deviation / sample mean x 100, where the sample mean is the BL signal obtained from ten micro-molds containing three-day-old HepG2 microtissues incubated with doxorubicin 1.0 µM for 18 hrs.

2.4 Hypoxia sensing in spherical microtissue

HEK293T cells were grown routinely in 5% CO_2 in air in minimum essential medium with Earle's salts (DMEM) supplemented with 10% (v/v) fetal bovine serum, 2 mM L-glutamine, 0.1 mM non-essential amino acids, MEM vitamins, and antibiotic/antimycotic solution.

Cells, previously seeded in a flat-bottom clear 24-well plate at a density of 8.0×10^4 cells/well, were transiently transfected with pGL4.42[luc2P/HRE/Hygro], using the FUGENE® HD transfection reagent at a ratio of 1:3.0 and incubated under standard conditions for 24 h at 37 °C and 5% CO_2. To obtain 3D spherical microtissue, the same procedure reported in the "*2.3 Tumoral sensing in spherical microtissue*". After spherical microtissue formation, cells were treated with 1,10 phenanthroline (concentration range from 0.1 to 100 µM) and incubated for 5 h in standard conditions (37°C, 5% CO_2). The half maximal effective concentration (EC_{50}), which is the concentration of the 1,10-phenanthroline producing 50% of the maximum response, was calculated using the equation: Y = Bottom + (Top − Bottom)/(1 + 10^((LogEC50 − X) × Hillslope)), where X is the logarithmic concentration of 1,10-phenanthroline. LOD and LOQ were calculated as the 1,10-phenanthroline

concentration that corresponded to the blank plus three times and ten times the standard deviation, respectively. All measurements were performed in triplicate and repeated with different cell at least three times.

Repeatability performance of the 3D tumoral sensing assay was calculated as Coefficient of Variation (CV%) = standard deviation / sample mean x 100, where the sample mean is the BL signal obtained from a number of ten micro-molds containing one-day-old Hek293T microtissues incubated with 1,10-phenanthroline 15.0 µM for 5 hrs.

3. Result and Discussions

To address the need of low-cost and sustainable bioassays for the assessment of multiple bioactivities to be used in different settings, from drug screening to agro-food industrial waste bioactivity monitoring, we developed a novel strategy for cell-based assays based on a 3D-printed microtissue device. We selected the monitoring of hypoxia and p53 pathways because a decrease in oxygen bioavailability in living cells triggers an adaptive cellular response to survive , unless this becomes severe and causes cell death. Depending on the cell line, the severity and the duration of hypoxia, oxygen deficiency influences p53 protein level and the modulation of the p53 pathway. To this end novel microtissue-based bioassays have been developed exploiting organ-on-a-chip technology to monitor hypoxia and p53 tumor suppressor pathways. Spherical microtissues have been obtained thanks to a low-cost and sustainable microfluidic chip previously developed by us [29]. This device was designed to comply with the FAIR's principles (findability, accessibility, interoperability, and reusability) and it proved to be suitable for repurposing via 3D printing and for easy integration with portable light detectors (CMOS camera) for point-of-need analysis, compatible with commercial benchtop instrumentation, low-cost and low carbon footprint (Figure S1).

The analytical procedure to obtain hypoxia and tumoral sensing microtissues is very simple and involves firstly the transient transfections of cells to express the Luc2P luciferase under the control of inducible promoters in accordance with the molecular pathway of interest, and then the obtainment of BL microtissues in an agarose support obtained in the microfluidic chip device. After 3D microtissues formation, 3D spherical microtissues are incubated with model compounds able to activate the molecular pathways and bioluminescence measurement can be performed with a conventional luminometer. The holder size allows easy manipulation and transfer of the scaffold free support in a conventional 24-well microplate for BL analysis, even in multiplex format with band pass filters and with low light intensities [29] (Figure 1).

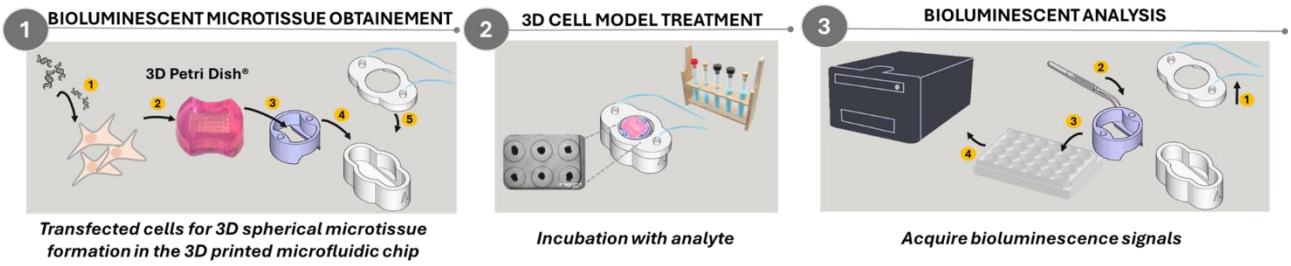

Figure 1: Schematic representation of the obtainment of BL 3D microtissues exploiting the low-cost and sustainable 3D printed microfluidic chip and BL analysis for monitoring specific bioactivities.

Before exploring this configuration, we characterized the luciferase Luc2P from *Photinus pyralis* in HEK293T cells transiently transfected with the pCDNA3.1_Luc2P vector and grown in 2D monolayer; kinetic emissions and spectra were obtained using the non-lysing D-LH_2 substrate and the commercial BrightGlo substrate. The selection of destabilized version of the Luc2P reporter protein was motivated by the need to monitor small and rapid changes in gene expression. Despite the red-shifting (λ_{max} = 623 nm) observed with the non-lysing D-LH_2 substrate (Figure S2), which is an asset in 3D cell models and *in vivo* imaging applications, we selected the lysing commercial BrightGlo

substrate which produced a BL signal 28 times higher than that obtained with the D-LH_2 (Figure S4). In addition, Luc2P showed a flash type emission kinetic with a peak after 3 min using the D-LH_2 substrate, while the characteristic glow-type emission kinetic was obtained with the BrightGlo susbstrate (Figure S3).

3.1 Bioluminescence for tumoral sensing in spherical microtissue

Three-day-old HepG2 microtissues, having an average diameter of 220 ± 20 µm (Figure 2), previously transfected with the reporter constructs pGL4.38[luc2P/p53 RE/Hygro], in which the Luc2P luciferase was placed under the control of the p53 promoter, were incubated in the micromolds with different concentrations of doxorubicin (from 0.1 to 5.0 µM) for 18 h at 37°C and 5% CO_2 [32].

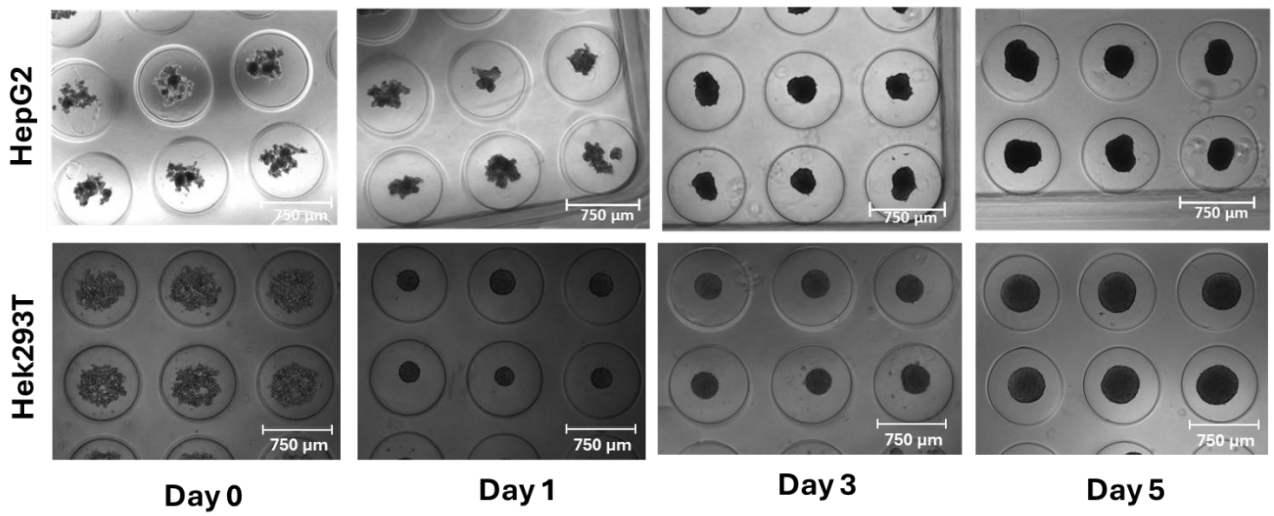

Figure 2: Growth monitoring of 3D spherical microtissues of HEK293T and HepG2 cells obtained with the microfluidic chip. Brightfield images were acquired with Thermo Scientific Invitrogen Evos M5000 Imaging Systems using a 4× objective.

BL emission kinetics of the 3D tumoral sensing microtissues were obtained after the addition of 50 µL BrightGlo substrate, and dose-response curves for doxorubicin with 18 h incubation period were

obtained and compared with those obtained from the 2D monolayer cultures. As shown in Figure 3 LODs of 0.43 and 0.62 µM were obtained for 2D cell cultures and microtissues, respectively, at 18 h incubation and an EC_{50} values of 0.7 ± 0.2 and 1.1 ± 0.3 µM, respectively. A LOQ of 0.5 µM was obtained in 2D cell-based assay and an LOQ of 0.9 µM in 3D spherical microtissues (Table S1). These ranges of concentration are relevant considering that the reported doxorubicin hematic after administration are between 0.025 and 0.250 µmol/L [33].

In 3D models an increase of BL as fold response over control proportional to the doxorubicin concentrations was also observed. Conversely in 2D cell-based assay higher doxorubicin concentrations of 1 µM have shown a proportional decrease in BL signals with a fold response of about 6.2, 2.8 and 0.2 for 1.50, 2.50 and 5.0 µM, respectively. Repeatability measurements were also performed in 3D models with a CV% of about 19%.

This confirms also the tendency of 2D cell-based assays to overestimate the efficacies of chemotherapeutic drugs compared with 3D models [34, 35] that show greater resistance to doxorubicin [36].

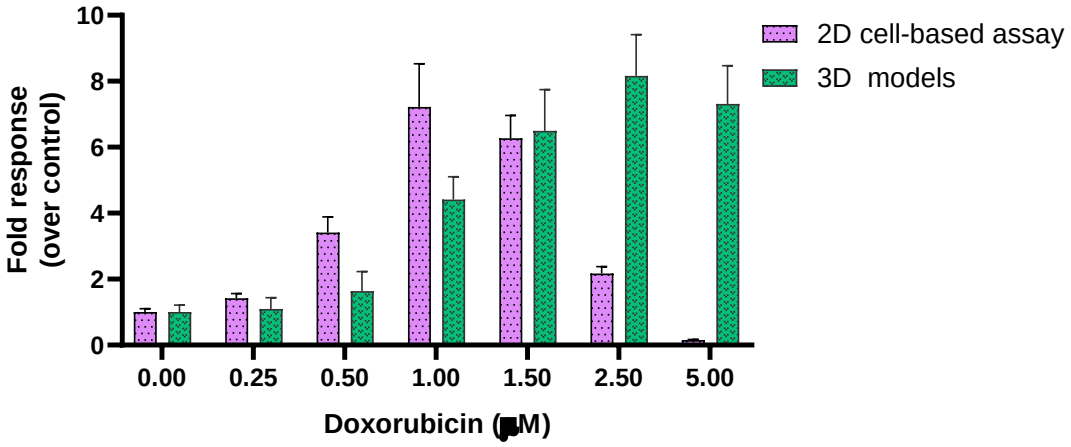

Figure 3: Doxorubicin dose-response curves obtained HepG2 genetically engineered with the plasmid reporter pGL4.38[luc2P/p53 RE/Hygro] and grown in 2D cell culture and 3D models. BL intensities were obtained with the Varioskan™ LUX multimode microplate.

In addition, as previously reported by Azimi et al. MDAMB231 cells grown in 2D format showed a significant decrease in viability when compared to that obtained with 3D models incubated with 5 µM of DOX [37].

3.2 Bioluminescence for hypoxia sensing in spherical microtissue

One-day-old HEK293T microtissues, having an average diameter of 180 ± 20 µm (Figure 2), and previously transfected in the 2D monolayer with the reporter constructs pGL4.42[luc2P/HRE/Hygro], in which the Luc2P luciferase was placed under the control of the HRE promoter, were incubated in the micromolds with different concentrations of 1,10-phenanthroline (from 0.1 to 100 µM) for 18 and 5 hrs at 37°C % and 5% CO_2. BL emission kinetics of the 3D tumoral sensing microtissues were obtained after the addition of 50 µL BrightGlo substrate.

The 1,10-phenanthroline mimics the effect of a reduced-oxygen environment on hypoxia-regulated promoter activity [38] through a mechanism HIF-1α-dependent. Under normoxic conditions, hypoxia can be activated by divalent metal ions [39] and by iron chelators such as desferrioxamine (DFO) [40]. Maxwell at el [39] reported the activity of the 1,10-phenanthroline as iron chelator [41] influencing the regular activity of dioxygenases by depriving cells of the essential free ferrous ions.

As shown in Figure 4, LODs of 0.52 and 3.37 µM were obtained for 2D cell cultures and microtissues, respectively, at 5 h incubation and EC_{50} values of 10.1 ± 0.5 and 14.5 ± 0.4 µM were obtained, respectively. EC_{50} values are consistent with those previously reported in 2D cell models with ME-

180 cells stably expressing a β-lactamase reporter gene under the regulation of an HRE (EC_{50}: 8.2 ± 0.7µM), supporting that 1,10 phenanthroline is one of the most potent inducers of HIF-1 [42]. LOQs of 1.5 and 4.6 µM were also obtained for 2D cell culture and 3D microtissues, respectively (Table S1) and a CV% of about 16% was also obtained for 3D models.

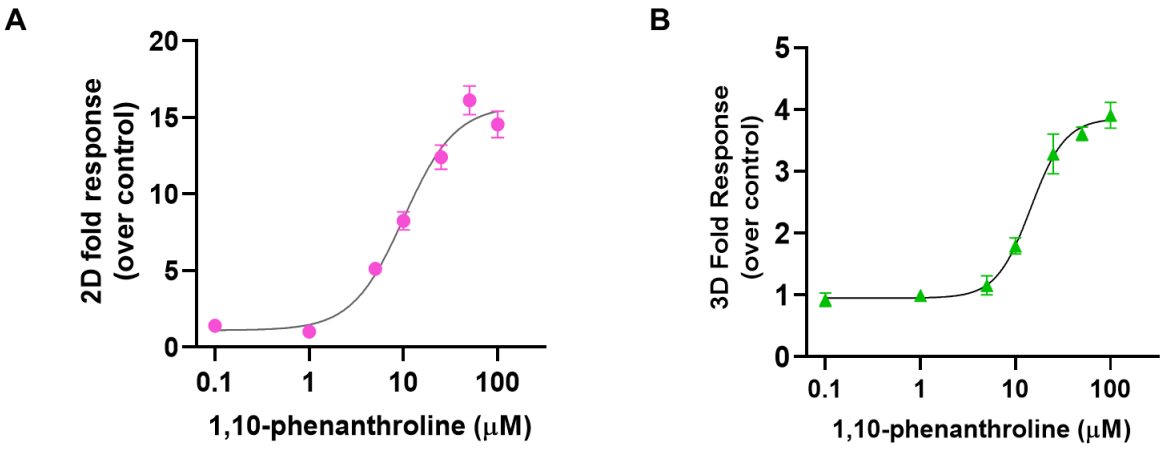

Figure 4: Dose-response curves for 1,10-phenanthroline obtained in HEK293T transfected with the reporter plasmid pGL4.42[luc2P/HRE/Hygro] and grown in 2D cell culture (A) and 3D models (B). BL intensities were obtained with the Varioskan™ LUX multimode microplate.

No significant cytotoxicity was observed in 2D and 3D models after incubation with 1,10-phenantroline for 5 h, despite half-maximal inhibitory concentration (IC_{50}) values were previously reported in the low micromolar range in ovarian A3780, breast MCF7 and cervical HeLa cell lines (48 h of incubation time) [43].

4. Conclusions

In this work, we report the development of novel bioassays to assess HIF and p53 pathway activations in 3D spherical microtissues obtained with a low-cost and sustainable chip platform. 3D microtissues were obtained with genetically engineered HEK293T and HepG2 3D cell models, exploiting Luc2P

luciferase as sensitive BL reporter for quantitative assessment of HIF and p53 pathways activations, respectively. The analytical performances were evaluated with model compounds, 1,10-phenanthroline for HIF activations and doxorubicin for p53 pathways activation, confirming the suitability of the proposed bioassays as valuable analytical tools for bioactivity analysis and drug screening. This could meet the need of pharmaceutical industries to obtain predictive information and to select pure molecules, active ingredients, food by-products, as promising therapeutics in human diseases, including different cancer types, acting on p53 regulation and HIF signalling.

Acknowledgments

This study was, in part, carried out within the Agritech National Research Center and received funding from the European Union Next-Generation EU National Recovery and Resilience Plan (NRRP), Mission 04 Component 2, investment 1.4—D.D. 1032 June 17, 2022, CN00000022 and investment 1.5—NextGenerationEU, call for tender no. 3277, dated 30/12/2021 and award number: 0001052, dated 23/06/2022. Part of the work was also funded by the European Union's Horizon Europe project FARMWISE under GA No. 101135533**.**

Declarations

Conflict of interest: The authors declare no competing interests.

Author contributions: M.M.C.: conceptualisation, investigation, methodology, formal analysis, data curation, validation, writing — original draft, review and editing; M.F.: investigation; A.T.: writing — review and editing, resources; S.M.: methodology; E.M.: conceptualization, methodology, validation, resources, writing — review and editing, supervision, funding.

References

1. (1960) The Principles of Humane Experimental Technique. Medical Journal of Australia 1:500–500. https://doi.org/10.5694/j.1326-5377.1960.tb73127.x

2. Calabretta MM, Michelini E (2024) Current advances in the use of bioluminescence assays for drug discovery: an update of the last ten years. Expert Opin Drug Discov 19:85–95. https://doi.org/10.1080/17460441.2023.2266989

3. Lenin S, Ponthier E, Scheer KG, Yeo ECF, Tea MN, Ebert LM, Oksdath Mansilla M, Poonnoose S, Baumgartner U, Day BW, Ormsby RJ, Pitson SM, Gomez GA (2021) A Drug Screening Pipeline Using 2D and 3D Patient-Derived In Vitro Models for Pre-Clinical Analysis of Therapy Response in Glioblastoma. Int J Mol Sci 22:4322. https://doi.org/10.3390/ijms22094322

4. Prince E, Kheiri S, Wang Y, Xu F, Cruickshank J, Topolskaia V, Tao H, Young EWK, McGuigan AlisonP, Cescon DW, Kumacheva E (2022) Microfluidic Arrays of Breast Tumor Spheroids for Drug Screening and Personalized Cancer Therapies. Adv Healthc Mater 11:. https://doi.org/10.1002/adhm.202101085

5. Żuchowska A, Baranowska P, Flont M, Brzózka Z, Jastrzębska E (2024) Review: 3D cell models for organ-on-a-chip applications. Anal Chim Acta 1301:342413. https://doi.org/10.1016/j.aca.2024.342413

6. Totaro G, Sisti L, Vannini M, Marchese P, Tassoni A, Lenucci MS, Lamborghini M, Kalia S, Celli A (2018) A new route of valorization of rice endosperm by-product: Production of polymeric biocomposites. Compos B Eng 139:195–202. https://doi.org/10.1016/j.compositesb.2017.11.055

7. Asma ST, Acaroz U, Imre K, Morar A, Shah SRA, Hussain SZ, Arslan-Acaroz D, Demirbas H, Hajrulai-Musliu Z, Istanbullugil FR, Soleimanzadeh A, Morozov D, Zhu K, Herman V, Ayad A, Athanassiou C, Ince S (2022) Natural Products/Bioactive Compounds as a Source of Anticancer Drugs. Cancers (Basel) 14:6203. https://doi.org/10.3390/cancers14246203

8. Mármol I, Quero J, Ibarz R, Ferreira-Santos P, Teixeira JA, Rocha CMR, Pérez-Fernández M, García-Juiz S, Osada J, Martín-Belloso O, Rodríguez-Yoldi MJ (2021) Valorization of agro-food by-products and their potential therapeutic applications. Food and Bioproducts Processing 128:247–258. https://doi.org/10.1016/j.fbp.2021.06.003

9. https://www.un.org/sustainabledevelopment/sustainable-consumption-production/

10. Socas-Rodríguez B, Álvarez-Rivera G, Valdés A, Ibáñez E, Cifuentes A (2021) Food by-products and food wastes: are they safe enough for their valorization? Trends Food Sci Technol 114:133–147. https://doi.org/10.1016/j.tifs.2021.05.002

11. Mohammadnezhad P, Valdés A, Álvarez-Rivera G (2023) Bioactivity of food by-products: an updated insight. Curr Opin Food Sci 52:101065. https://doi.org/10.1016/j.cofs.2023.101065

12. Rather RA, Bhagat M (2020) Quercetin as an innovative therapeutic tool for cancer chemoprevention: Molecular mechanisms and implications in human health. Cancer Med 9:9181–9192. https://doi.org/10.1002/cam4.1411

13. Nagle D, Zhou Y-D (2006) Natural Product-Based Inhibitors of Hypoxia-Inducible Factor-1 (HIF-1). Curr Drug Targets 7:355–369. https://doi.org/10.2174/138945006776054979

14. Zhang C, Liu J, Wang J, Zhang T, Xu D, Hu W, Feng Z (2021) The Interplay Between Tumor Suppressor p53 and Hypoxia Signaling Pathways in Cancer. Front Cell Dev Biol 9:. https://doi.org/10.3389/fcell.2021.648808

15. Wicks EE, Semenza GL (2022) Hypoxia-inducible factors: cancer progression and clinical translation. Journal of Clinical Investigation 132:. https://doi.org/10.1172/JCI159839

16. Petrova V, Annicchiarico-Petruzzelli M, Melino G, Amelio I (2018) The hypoxic tumour microenvironment. Oncogenesis 7:10. https://doi.org/10.1038/s41389-017-0011-9

17. Choueiri TK, Kaelin WG (2020) Targeting the HIF2–VEGF axis in renal cell carcinoma. Nat Med 26:1519–1530. https://doi.org/10.1038/s41591-020-1093-z

18. Zhang C, Liu J, Xu D, Zhang T, Hu W, Feng Z (2020) Gain-of-function mutant p53 in cancer progression and therapy. J Mol Cell Biol 12:674–687. https://doi.org/10.1093/jmcb/mjaa040

19. Hsu C-W, Huang R, Khuc T, Shou D, Bullock J, Grooby S, Griffin S, Zou C, Little A, Astley H, Xia M (2016) Identification of approved and investigational drugs that inhibit hypoxia-inducible factor-1 signaling. Oncotarget 7:8172–8183. https://doi.org/10.18632/oncotarget.6995

20. Aggarwal V, Miranda O, Johnston PA, Sant S (2020) Three dimensional engineered models to study hypoxia biology in breast cancer. Cancer Lett 490:124–142. https://doi.org/10.1016/j.canlet.2020.05.030

21. Cevenini L, Calabretta MM, Lopreside A, Tarantino G, Tassoni A, Ferri M, Roda A, Michelini E (2016) Exploiting NanoLuc luciferase for smartphone-based bioluminescence cell biosensor for (anti)-inflammatory activity and toxicity. Anal Bioanal Chem 408:8859–8868. https://doi.org/10.1007/s00216-016-0062-3

22. Lopreside A, Calabretta MM, Montali L, Ferri M, Tassoni A, Branchini BR, Southworth T, D'Elia M, Roda A, Michelini E (2019) Prêt-à-porter nanoYESα and nanoYESβ bioluminescent cell biosensors for ultrarapid and sensitive screening of endocrine-disrupting chemicals. Anal Bioanal Chem 411:4937–4949. https://doi.org/10.1007/s00216-019-01805-2

23. Kirchherr J, Reike D, Hekkert M (2017) Conceptualizing the circular economy: An analysis of 114 definitions. Resour Conserv Recycl 127:221–232. https://doi.org/10.1016/j.resconrec.2017.09.005

24. Cevenini L, Calabretta MM, Calabria D, Roda A, Michelini E (2015) Luciferase Genes as Reporter Reactions: How to Use Them in Molecular Biology? pp 3–17

25. D'Alessandro S, Camarda G, Corbett Y, Siciliano G, Parapini S, Cevenini L, Michelini E, Roda A, Leroy D, Taramelli D, Alano P (2016) A chemical susceptibility profile of the *Plasmodium falciparum* transmission stages by complementary cell-based gametocyte assays. Journal of Antimicrobial Chemotherapy 71:1148–1158. https://doi.org/10.1093/jac/dkv493

26. Lopreside A, Montali L, Wang B, Tassoni A, Ferri M, Calabretta MM, Michelini E (2021) Orthogonal paper biosensor for mercury(II) combining bioluminescence and colorimetric smartphone detection. Biosens Bioelectron 194:113569. https://doi.org/10.1016/j.bios.2021.113569

27. Calabretta MM, Gregucci D, Michelini E (2023) New synthetic red- and orange-emitting luciferases to upgrade *in vitro* and 3D cell biosensing. Analyst 148:5642–5649. https://doi.org/10.1039/D3AN01251D

28. Calabretta M, Gregucci D, Martínez-Pérez-Cejuela H, Michelini E (2022) A Luciferase Mutant with Improved Brightness and Stability for Whole-Cell Bioluminescent Biosensors and In Vitro Biosensing. Biosensors (Basel) 12:742. https://doi.org/10.3390/bios12090742

29. Calabretta MM, Gregucci D, Guardigli M, Michelini E (2024) Low-cost and sustainable smartphone-based tissue-on-chip device for bioluminescence biosensing. Biosens Bioelectron 261:116454. https://doi.org/10.1016/j.bios.2024.116454

30. Wang Y, Gao Y, Pan Y, Zhou D, Liu Y, Yin Y, Yang J, Wang Y, Song Y (2023) Emerging trends in organ-on-a-chip systems for drug screening. Acta Pharm Sin B 13:2483–2509. https://doi.org/10.1016/j.apsb.2023.02.006

31. Calabretta MM, Lopreside A, Montali L, Zangheri M, Evangelisti L, D'Elia M, Michelini E (2022) Portable light detectors for bioluminescence biosensing applications: A comprehensive review from the analytical chemist's perspective. Anal Chim Acta 1200:339583. https://doi.org/10.1016/j.aca.2022.339583

32. McSweeney KM, Bozza WP, Alterovitz W-L, Zhang B (2019) Transcriptomic profiling reveals p53 as a key regulator of doxorubicin-induced cardiotoxicity. Cell Death Discov 5:102. https://doi.org/10.1038/s41420-019-0182-6

33. Linders AN, Dias IB, López Fernández T, Tocchetti CG, Bomer N, Van der Meer P (2024) A review of the pathophysiological mechanisms of doxorubicin-induced cardiotoxicity and aging. npj Aging 10:9. https://doi.org/10.1038/s41514-024-00135-7

34. Karlsson H, Fryknäs M, Larsson R, Nygren P (2012) Loss of cancer drug activity in colon cancer HCT-116 cells during spheroid formation in a new 3-D spheroid cell culture system. Exp Cell Res 318:1577–1585. https://doi.org/10.1016/j.yexcr.2012.03.026

35. Fontoura JC, Viezzer C, dos Santos FG, Ligabue RA, Weinlich R, Puga RD, Antonow D, Severino P, Bonorino C (2020) Comparison of 2D and 3D cell culture models for cell growth, gene expression and drug resistance. Materials Science and Engineering: C 107:110264. https://doi.org/10.1016/j.msec.2019.110264

36. Yip D, Cho CH (2013) A multicellular 3D heterospheroid model of liver tumor and stromal cells in collagen gel for anti-cancer drug testing. Biochem Biophys Res Commun 433:327–332. https://doi.org/10.1016/j.bbrc.2013.03.008

37. Azimi T, Loizidou M, Dwek M V. (2020) Cancer cells grown in 3D under fluid flow exhibit an aggressive phenotype and reduced responsiveness to the anti-cancer treatment doxorubicin. Sci Rep 10:12020. https://doi.org/10.1038/s41598-020-68999-9

38. Xia M, Huang R, Sun Y, Semenza GL, Aldred SF, Witt KL, Inglese J, Tice RR, Austin CP (2009) Identification of Chemical Compounds that Induce HIF-1α Activity. Toxicological Sciences 112:153–163. https://doi.org/10.1093/toxsci/kfp123

39. Maxwell P, Salnikow K (2004) HIF-1, An Oxygen and Metal Responsive Transcription Factor. Cancer Biol Ther 3:29–35. https://doi.org/10.4161/cbt.3.1.547

40. Wang GL, Semenza GL (1993) General involvement of hypoxia-inducible factor 1 in transcriptional response to hypoxia. Proceedings of the National Academy of Sciences 90:4304–4308. https://doi.org/10.1073/pnas.90.9.4304

41. Rauen U, Springer A, Weisheit D, Petrat F, Korth H, de Groot H, Sustmann R (2007) Assessment of Chelatable Mitochondrial Iron by Using Mitochondrion-Selective Fluorescent Iron Indicators with Different Iron-Binding Affinities. ChemBioChem 8:341–352. https://doi.org/10.1002/cbic.200600311

42. Xia M, Huang R, Sun Y, Semenza GL, Aldred SF, Witt KL, Inglese J, Tice RR, Austin CP (2009) Identification of Chemical Compounds that Induce HIF-1α Activity. Toxicological Sciences 112:153–163. https://doi.org/10.1093/toxsci/kfp123

43. Matos CP, Addis Y, Nunes P, Barroso S, Alho I, Martins M, Matos APA, Marques F, Cavaco I, Costa Pessoa J, Correia I (2019) Exploring the cytotoxic activity of new phenanthroline salicylaldimine Zn(II) complexes. J Inorg Biochem 198:110727. https://doi.org/10.1016/j.jinorgbio.2019.110727

Supporting materials

Novel bioassays based on 3D-printed device for sensing of hypoxia and p53 pathway in 3D cell models

Maria Maddalena Calabretta[a,b*], Maura Ferri[c], Annalisa Tassoni[c], Stefania Maiello[a], Elisa Michelini[a,b,d*]

[a]*Department of Chemistry "Giacomo Ciamician", University of Bologna, Via P. Gobetti 85, 40129, Bologna, Italy*

[b]*Center for Applied Biomedical Research (CRBA), Azienda Ospedaliero-Universitaria Policlinico S. Orsola-Malpighi, 40138 Bologna, Italy*

[c]*Department of Biological, Geological and Environmental Sciences, University of Bologna, Bologna, Italy*

[d]*Health Sciences and Technologies Interdepartmental Center for Industrial Research (HSTICIR), University of Bologna, 40126, Bologna, Italy*

*Corresponding authors:

Prof. Elisa Michelini

University of Bologna

Dept. of Chemistry "Giacomo Ciamician"

Via P. Gobetti 85, 40129 Bologna, Italy

elisa.michelini8@unibo.it

Dr. Maria Maddalena Calabretta

University of Bologna

Dept. of Chemistry "Giacomo Ciamician"

Via P. Gobetti 85, 40129 Bologna, Italy

maria.calabretta2@unibo.it

Table of contents

Figure S1: 3D printed microfluidic chip components (cover, container and holder) obtained with Formlabs 3D printer.

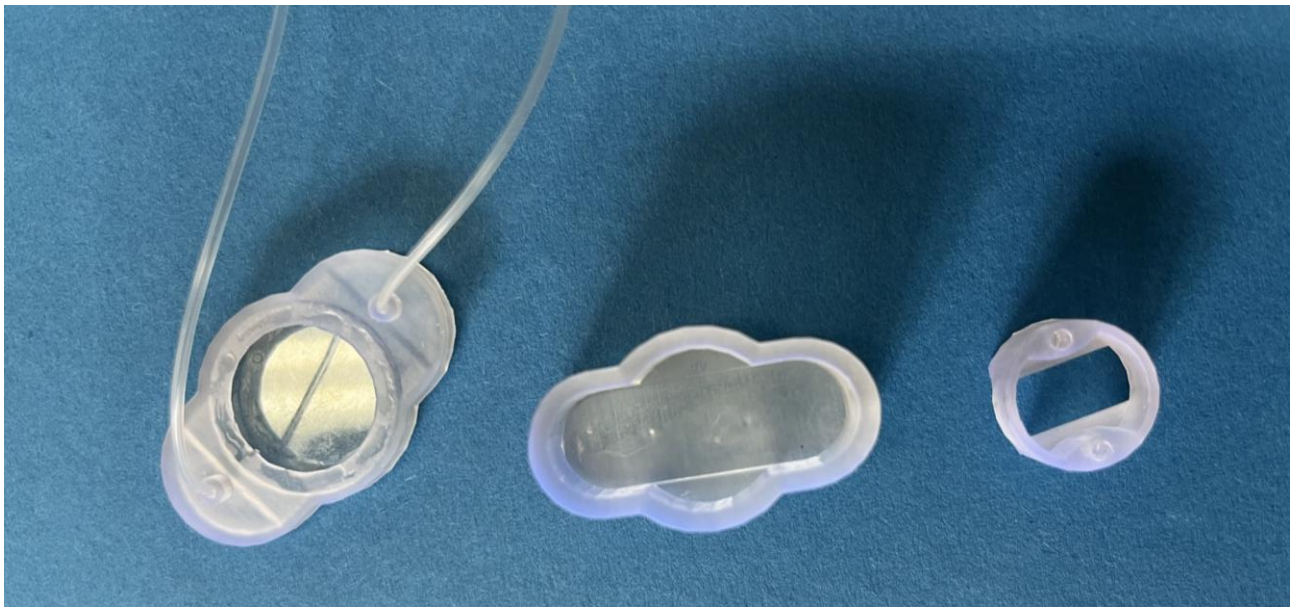

Figure S2: Emission spectra of Luc2P luciferase obtained in HEK293T genetically engineered to express constitutively Luc2P luciferase using the commercial lysing BrightGlo substrate and the D-LH_2 substrate in citrate buffer (1.0 mM, pH 5.0).

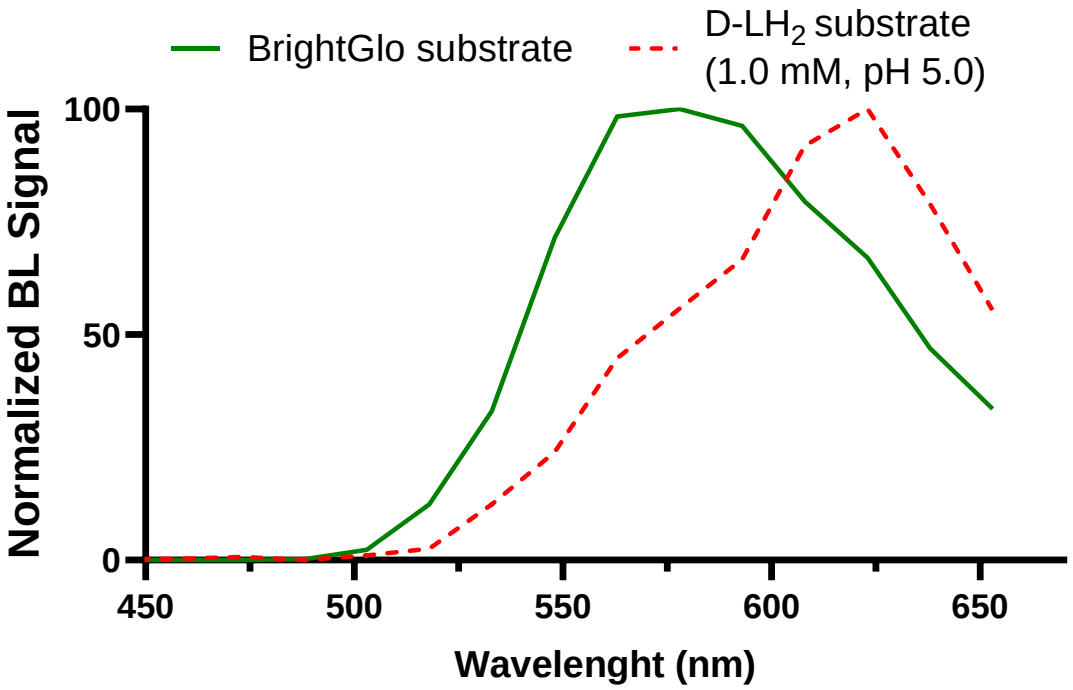

Figure S3: Kinetic emissions of HEK293T genetically engineered to express constitutively Luc2P luciferase using the commercial lysing BrightGlo substrate and the D-LH_2 substrate in citrate buffer (1.0 mM, pH 5.0).

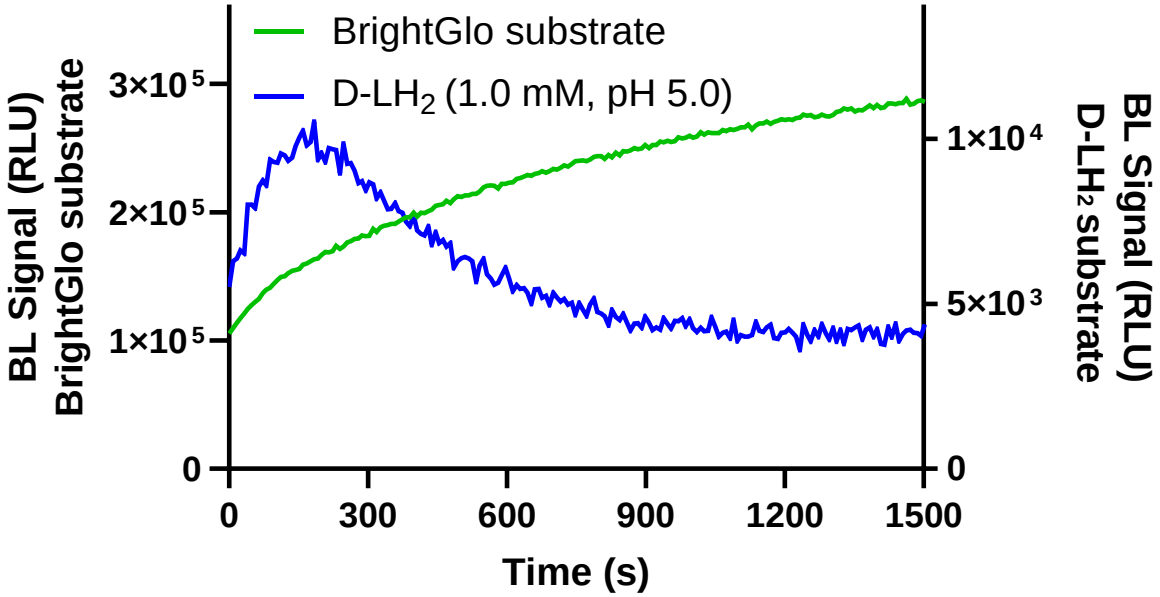

Figure S4: Maximum bioluminescent intensities of HEK293T genetically engineered to express constitutively Luc2P luciferase obtained with the BrightGlo substrate and the D-LH_2 substrates.

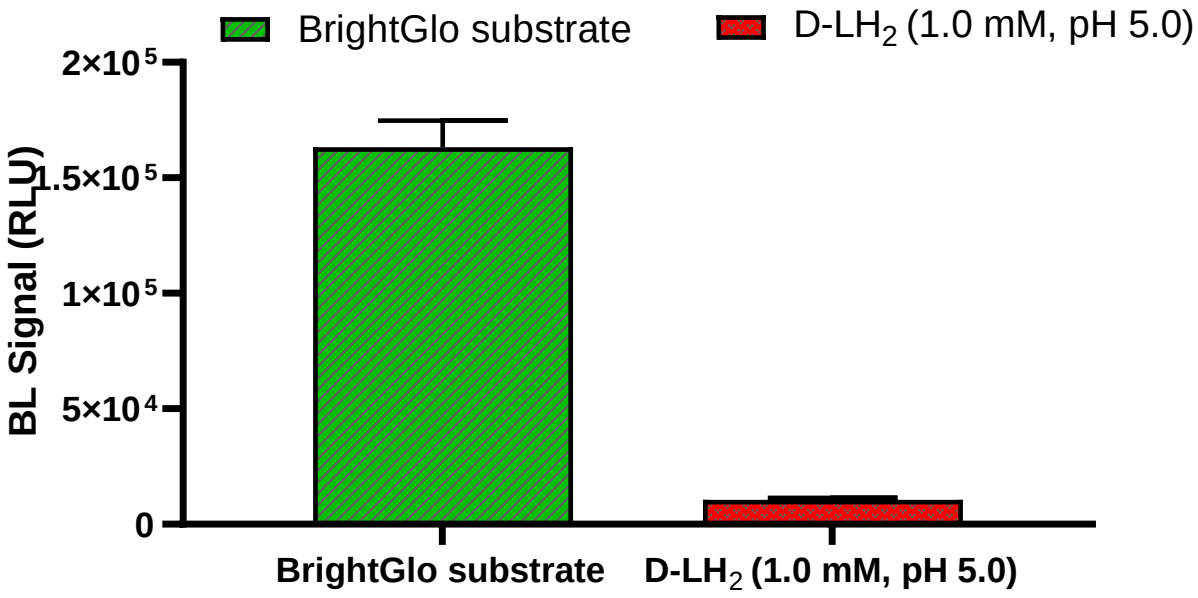

Table S1: Analytical performance of the hypoxia and tumoral sensing assays

	Hypoxia sensing assay (1,10-phenatroline)		Tumoral sensing assay (doxorubicin)	
	2D	**3D**	**2D**	**3D**
LOD	0.52 µM	3.37 µM	0.43 µM	0.62 µM
LOQ	1.5 µM	4.6 µM	0.5 µM	0.9 µM
EC_{50}	10.1 ± 0.5 µM	14.5 ± 0.4 µM	0.7 ± 0.2 µM	1.1 ± 0.3 µM
Concentration range	1.5 – 50.0 µM	4.6 – 100.0 µM	0.5 -1.0 µM	0.9 – 5.0 µM